Journal of Environmental Pathology, Toxicology and Oncology, 20(Suppl. 1):67–74 (2001)

IgG Subclass Responses in Experimental Silicosis

David N. Weissman,[1] Ann F. Hubbs,[1] Shu-Hai Huang,[2] Charles F. Stanley,[3] Yongyut Rojanasakul,[3] & Joseph K. H. Ma[3]

Silicosis is a crippling fibrotic lung disease induced by inhaling crystalline silica. In addition to fibrosis, silica inhalation by humans is associated with a number of immunological effects including increased levels of serum immunoglobulins (in particular IgG), increased prevalence of autoantibodies, and autoimmune disease. Recent studies using rodent models have shown that experimental silicosis is associated with a T-helper (T_H)1 pattern of T-cell activation in the lungs and lung-associated lymph nodes after silica inhalation, which are also the sites of increased IgG production. We therefore hypothesized that the subclass distribution of IgG production occurring in experimental silicosis would suggest T_H1 activation as the primary stimulus for IgG production. Using an ELISPOT assay, we found increased IgG-secreting spot-forming cells of all IgG subclasses in lung-associated lymph nodes taken from silica-exposed rats 3 to 4 months after aerosol exposure to silica. Neither T_H1- nor T_H2-dependent IgG subclass-secreting cells were selectively enhanced. Our findings suggest that T_H1 activation alone does not account for increased production of IgG in experimental silicosis.

KEY WORDS: silicosis, quartz, IgG, lymphocyte, cytokine, lung

Introduction

Silicosis is a crippling lung disease induced by inhalation of crystalline silica.[1] Chronic silicosis develops over a period of years, as retained intrapulmonary crystalline silica induces a sequence of events including inflammation, production and deposition of extracellular matrix proteins, and, ultimately, end-stage pulmonary fibrosis.[2-4] Stimulation of macrophages by silica and subsequent cytokine networking between macrophages, lymphocytes, neutrophils, fibroblasts, and potentially other cell types is an important mechanism for fibroblast stimulation and the development of pulmonary fibrosis.[5-8]

An additional likely result of silica-induced cytokine networking not necessarily underlying fibrosis is immune dysfunction, both systemic and in the lung.[4-9] Clinical manifestations of immunologic dysfunction associated with chronic silicosis include autoimmune diseases, such as progressive systemic sclerosis, increased prevalence of autoantibodies, and

[1]Health Effects Laboratory Division, National Institute for Occupational Safety and Health, Morgantown, WV; [2]Guangxi Institute of Occupational Disease, Nanning, P. R. China; [3]West Virginia University, Morgantown, WV. Correspondence: David N. Weissman, M.D., National Institute for Occupational Safety and Health, Health Effects Laboratory Division, Analytical Services Branch, 1095 Willowdale Rd., Morgantown WV 26505. dqw4@cdc.gov.

Acknowledgments: The authors would like to thank Dr. David Frazier and Mr. Travis Goldsmith for their assistance in particle characterization, and Zhenzhen Zhuang for her excellent technical support. This work was partially supported by the US Bureau of Mines, Generic Mineral Technology Center for Respiratory Dust.

0731-8898/01/$5.00

increased susceptibility to pulmonary mycobacterial infections, such as tuberculosis.

A proposed mechanism for silica-associated immune dysfunction is induction of a T-helper (T_H)1 pattern of lymphocyte activation within the lungs and lung-associated lymph nodes (LALN).[10-12] T_H1 lymphocyte activation has been documented in the lungs and LALN of silica-exposed mice[10,11] and in the LALN of silica-exposed rats.[12] In mice, intrapulmonary transcription and translation of the T_H1 cytokine interferon (IFN)-γ is increased in experimental silicosis. In rats, experimental silicosis leads to increased transcription and translation of IFN-γ within LALN, while transcription and translation of the T_H2 cytokine IL-10 is decreased.

In addition to T-lymphocyte activation, experimental silicosis in rats is also associated with B lymphocyte activation that is characterized by increased production of immunoglobulin, particularly IgG, within the lungs and LALN.[13] T-cell activation potentially underlies B-cell activation and IgG production, as T cells and their cytokines profoundly affect both level and subclass distribution of IgG production by B cells.[14,15] Cytokines regulate the distribution of IgG subclass production by selectively inducing transcriptional activation of the constant heavy (C_H) genes encoding particular subclass C_H regions. C_H gene activation in turn makes switch regions accessible to switch recombinases. In the mouse, the T_H1 cytokine IFN-γ preferentially induces production of IgG2a and, under certain conditions, IgG3 by B cells. The T_H2 cytokine IL-4 preferentially induces production of IgG1 and IgE.[15] The situation in the rat is less well characterized, but available data are consistent with T_H1 and T_H2 cells supporting different patterns of rat IgG subclass production.[16,17]

On the basis of these considerations, the major hypothesis underlying this study was that inhalation of crystalline silica would initiate a sequence of events leading not only to fibrosis, but also to immune dysfunction. Furthermore, that the subclass distribution of IgG response induced by experimental silicosis would be compatible with a T_H1 pattern of T-cell activation. Our findings showed increased serum IgG and increased secretion of IgG by cells from LALN and lungs in experimental silicosis. However, the pattern of IgG subclass production observed by us could not be accounted for solely by T_H1 activation.

Materials and Methods

Animals

Male Fischer F344 rats were purchased from Charles River Laboratories, Wilmington, MA, USA. Rats weighed 150–175 g upon arrival and were housed in filter-topped polycarbonate cages and kept in HEPA-filtered laminar flow animal isolators. Animals were allowed food and water ad libitum and held for 2 weeks prior to use. All protocols involving the use of animals were approved by the West Virginia University Institutional Animal Care and Use Committee.

Aerosol Exposures

Exposures were conducted as reported for a well documented experimental model of silicosis.[13] The model was specifically chosen for its ability to reproduce the pulmonary manifestations of human silicosis. Rats were exposed to aerosols of either α-quartz (Min-U-Sil <5; US Silica Products, Berkeley Springs, WV, USA) or diluent air 5 hours per day for 8 days (Tuesday–Friday, then Monday–Thursday). Exposures were performed in horizontal flow chambers and dusts were aerosolized using a TSI 9310 fluidized bed aerosol generator (TSI, St. Paul, MN, USA).[18] The exposure system generated silica aerosols at a concentration of 39 mg/m^3. Evaluation of the aerosol by cascade impactor documented that the mass median aerodynamic diameter (MMAD) of silica was 0.95 μm, with a geometric standard deviation of 1.7 μm.

Experimental Protocol

In general, responses to experimental silicosis were documented using two-way comparisons of findings in the silica- and air-exposed groups. Animals were evaluated at 3 to 4 months after exposure, a time interval after exposure to silica known to be associated with increased levels of serum IgG.[13] Induction of pulmonary inflammation was documented by evaluation of inflammatory parameters in bronchoalveolar lavage (BAL). Serum IgG response was documented by ELISA. Anatomic and subclass distributions of IgG-secreting cells after exposure to silica

was documented using an ELISPOT assay that enumerated cells making various IgG subclasses as IgG subclass spot-forming cells (SFC).[19] SFC were measured in the lung, LALN, and spleen.

Samples and Cell Populations

Rats were sacrificed by i.p. injection of Ketamine/Xylazine followed by cardiac exsanguination. Blood was saved and serum prepared from clotted blood. For each rat, two parathymic lymph nodes (referred to here as LALN and illustrated in Bice et al.[20]) were identified, removed, and placed together in cold RPMI 1640 supplemented with 25 mM HEPES, 50 μg/mL gentamycin and 2 mM L-glutamine (RPMI, Gibco, Grand Island, NY, USA). Lymph node cell populations were obtained by passing the lymph nodes through a dounce tissue homogenizer. Resulting cell suspensions were pelleted by centrifugation at 500× g for 10 minutes at 4 °C, washed twice in RPMI, and suspended in RPMI containing 10% heat-inactivated fetal calf serum (CRPMI, HyClone Laboratories, Logan, UT, USA).

Lungs were perfused with normal saline via the right ventricular outflow tract until oligemic. Animals were further exsanguinated by transection of the aorta. Bronchoalveolar lavage was performed by tracheal cannulation, followed by infusion of 5 mL normal saline and recovery by gentle suction. Five such aliquots were instilled and recovered. Lavage fluid recovered from each rat was centrifuged (500× g for 10 min), and the resulting cell pellet was resuspended in RPMI for determination of differential cell counts.

For animals used to measure pulmonary SFC, BAL was not performed. Instead, left lungs were removed, dissected free of major airway, rinsed with normal saline to remove residual blood, and finely minced in cold RPMI. Lung mince was dissociated into a cell suspension by passage through a stainless steel screen (Cellector, 100 mesh; Thomas Scientific, Swedesboro, NJ, USA). Cells were pelleted by centrifugation and washed twice in RPMI. Pulmonary interstitial cells were enriched for mononuclear cells by density gradient centrifugation (Histopaque-1083; Sigma Diagnostics, St. Louis, MO, USA). Cells at the gradient interface were harvested, washed twice in RPMI, and then suspended in CRPMI.

Spleen cell suspensions were made by pressing spleens between two microscope slides in a Petri dish filled with cold RPMI, and then suspending the cells released by repeated aspiration through a sterile Pasteur pipette. The resulting cell suspension was pelleted by centrifugation and then washed twice in RPMI. Splenic mononuclear cells were separated from contaminants such as red blood cells by density gradient centrifugation (Histopaque-1083, Sigma). Cells at the gradient interface were harvested, washed twice in RPMI, and then suspended in CRPMI.

Cell populations were enumerated using a Coulter Counter. Cell differentials were performed by counting cells on cytocentrifuge preparations stained with Diff-Quik® (American Scientific Products, McGaw Park IL, USA). Cell viabilities were determined by trypan blue exclusion.

Measurement of Serum IgG

IgG levels were measured in serum using a sandwich enzyme-linked immunosorbent assay (ELISA). Goat anti-rat IgG (1 μg/mL; Kirkegaard & Perry Laboratories, Gaithersburg, MD, USA) was used as a capture antibody. Standards were prepared from rat IgG (Sigma). Goat anti-rat IgG peroxidase conjugate diluted 1:250 in PBS/BSA (Kirkegaard & Perry) was used as a detecting antibody. The chromogenic substrate used was 2,2′-azino-di[3-ethyl-benzthiazoline sulfonate] (ABTS; Kirkegaard & Perry). Color development was measured using an automated ELISA plate reader at a wavelength of 405 nm (Bio-tek Instruments, Winooski, VT, USA) and immunoglobulin concentrations determined by comparison of sample color development to standard curves (Kineticalc, Bio-tek).

Quantification of B Cells

B-lymphocyte subpopulations of cells obtained from LALN were quantified by flow cytometry (FACScan, Becton Dickinson, San Jose, CA, USA). Immunofluorescence staining was performed using a fluorescein isothiocyanate (FITC)-conjugated monoclonal antibody (Clone OX-33; Pharmingen, San Diego, CA, USA). Lymphocyte populations were identified by forward and side scatter and percent

lymphocytes binding the monoclonal antibody by fluorescence intensity. Gate settings for analysis of fluorescence intensity were determined using cells stained with an irrelevant FITC-conjugated monoclonal antibody (Pharmingen).

Measurement of IgG-Secreting Cells by ELISPOT

Assays were performed in nitrocellulose-bottomed Millititer-HA plates (Millipore, Bedford, MA, USA). The following capture antibodies were used: goat antirat IgG (for IgG-SFC; Kirkegaard & Perry); mouse monoclonal antirat IgG1 (for IgG1-SPF; clone RG11/39.4), IgG2a (for IgG2a-SPF; clone RG7/1.30), or IgG2b (for IgG2b-SPF; clone RG7/11.1) (all from Pharmingen); or mouse monoclonal antirat IgG2c (for IgG2c-SPF; clone MARG2C-3) (Sigma). Plates were coated with capture antibodies diluted in Hank's balanced salt solution (HBSS), 100 μL/well, 4 °C, overnight. Next, plates were emptied and washed three times with HBSS and blocked with CRPMI, 100 μL/well, 37 °C, for 30 minutes. Wells were emptied and 100 μL cell suspension in CRPMI was added to each well. For IgG and each of the IgG subclasses, duplicate cultures were performed using each of the following number of cells per well: 2×10^5, 10^5, 5×10^4, and 10^4. Culture plates were incubated at 37 °C, 5% CO_2 for 4 hours. Cell suspensions were removed, the plates washed three times with PBS/Tween, and the membrane at the bottom of each plate was blotted dry. To visualize spots created on the membrane by individual IgG-secreting cells, plates were incubated with goat antirat IgG-alkaline phosphatase conjugate (Southern Biotechnology Associates, Birmingham, AL, USA), washed, and then incubated with the chromogenic substrate 5-bromo-4-chloro-3-indolyl phosphate/*p*-nitroblue tetrazolium salt (BCIP/NBT, Kirkegaard & Perry). Color development was watched and when spots were sufficiently developed, the plate was washed with water and allowed to dry. Spots were counted using a dissecting microscope and the results were expressed as SFC/10^4 cells.

Statistics

Results are expressed as means ± standard errors except where indicated. Two-way comparisons between silica-exposed and air-exposed groups were performed using unpaired *t* tests for normally distributed data or Mann-Whitney rank sum tests for data that were not normally distributed (Sigmastat statistical software, SPSS, Chicago, IL, USA). Differences were considered significantly different at a level of $p < 0.05$.

Results

Cell Populations Recovered After Silica or Air Exposure

Silica exposure markedly affected cell recoveries from lung and LALN, but not spleen (Table 1). LALN were especially affected. They were markedly enlarged and total cell recovery from LALN was increased almost 32-fold. In all cases, greater than 98% of LALN cells were lymphocytes. Silica exposure affected the relative percentage of LALN cells that were B cells. The percentage of LALN B cells in-

TABLE 1. Impact of Silica Exposure on Cell Recoveries[a]

	BAL	Lung	LALN	Spleen
Air	1.3 ± 0.2	3.7 ± 0.7	7.4 ± 1.5	54 ± 8
Silica	22.0 ± 3.0[b]	12.6 ± 2.4[b]	236 ± 18[b]	51 ± 9

Note: BAL, bronchoalveolar lavage; LALN, lung-associated lymph node. Values are $\times 10^6$.

[a] $n = 5$ per group for all comparisons.

[b] Silica and air groups different, <0.05.

creased significantly, from 16.4% ± 2.3% in air-exposed rats to 28.5% ± 1.2% in silica-exposed rats.

Silica exposure also affected the numbers and types of cells recovered from the lungs (Tables 1–3). BAL cells increased 17-fold, with an increased relative percentage of neutrophils and a decreased relative percentage of alveolar macrophages. However, because of the marked increase in the total numbers of cells recovered, the total numbers of alveolar macrophages, lymphocytes, and neutrophils were all significantly increased in BAL in the silica-exposed animals.

Silica exposure markedly affected the number and type of cells recovered from lung tissue after enzymatic digestion and density gradient centrifugation. The total number of cells recovered were increased 3.4-fold relative to saline controls (Table 1). Silica exposure was associated with an increased relative percentage of neutrophils, which came at the expense of a decreased relative proportion of lymphocytes (Table 3). However, because of the increase in the total number of cells recovered, the total number of all cell types recovered were significantly increased after silica exposure.

TABLE 2. Impact of Silica Exposure on BAL Cell Differentials

	AM (%)	Lymph (%)	PMN (%)
Air	88.4 ± 1.3	11.3 ± 1.2	0.3 ± 0.1
Silica	18.8 ± 0.9[a]	8.6 ± 1.5	72.6 ± 1.9[a]

Note: AM, alveolar macrophage; Lymph, lymphocytes; PMN, polymorphonuclear cells (neutrophils).
[a] Silica and air groups different, $p < 0.05$.

TABLE 3. Impact of Silica Exposure on Lung Mince Cell Differentials

	MAC (%)	Lymph (%)	PMN (%)
Air	52.9 ± 3.2	45.9 ± 3.5	1.2 ± 0.7
Silica	50.3 ± 2.2	19.1 ± 1.9*	30.4 ± 1.7*

Note: MAC, macrophages; lymph, lymphocytes; PMN, polymorphonuclear cells (neutrophils).
[a] Silica and air groups different, $p < 0.05$.

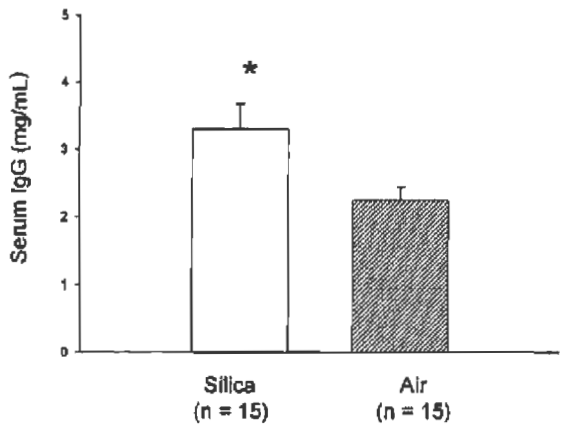

FIGURE 1. Serum IgG concentrations in silica- and air-exposed rats sacrificed 3–4 months after exposure. Each bar represents mean ± SEM of 15 experiments. *Silica and air groups different ($p < 0.05$).

IgG and IgG Subclass Responses to Silica or Air Exposure

Silica exposure was associated with a significant increase in serum IgG concentrations (Fig. 1). IgG-SFC were significantly increased in both LALN and lung cell populations of silica-exposed animals (Figs. 2 and 3). IgG-SFC were increased 24-fold in LALN cells (which were >98% lymphocytes) and 22-fold when normalized to lung lymphocytes.

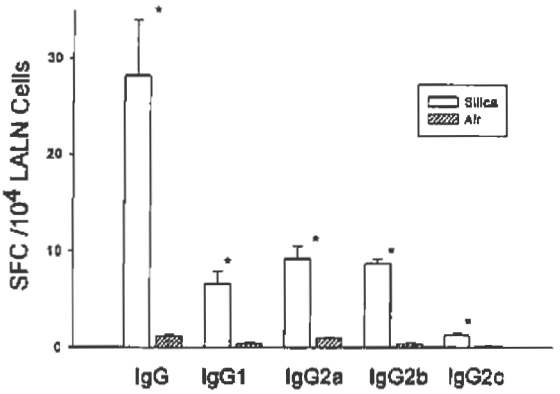

FIGURE 2. IgG and IgG subclass spot-forming cells (SFC) in lung-associated lymph node (LALN) cell populations of silica- and air-exposed rats sacrificed 3–4 months after exposure. Each bar represents mean ± SEM of five experiments. *Silica and air groups different ($p < 0.05$).

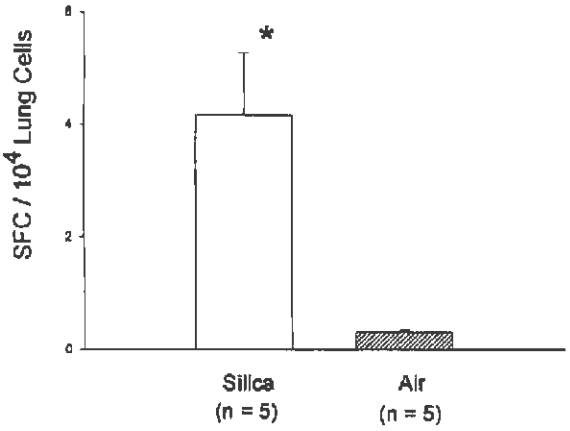

FIGURE 3. IgG spot-forming cells (SFC) in lung interstitial cell populations of silica- and air-exposed rats sacrificed 3–4 months after exposure. Each bar represents mean ± SEM of five experiments. *Silica and air groups different ($p < 0.05$).

SFC numbers for each of the IgG subclasses were significantly greater in LALN from silica-exposed than air-exposed animals (Fig. 2). IgG1-SFC were increased 18-fold; IgG2a-SFC, 10-fold; IgG2b-SFC, 28-fold; and IgG2c-SFC, 8-fold.

In contrast to lung and LALN, no significant increases in IgG-SFC or IgG subclass-SFC were noted in spleen-cell populations from silica-exposed rats (Fig. 4).

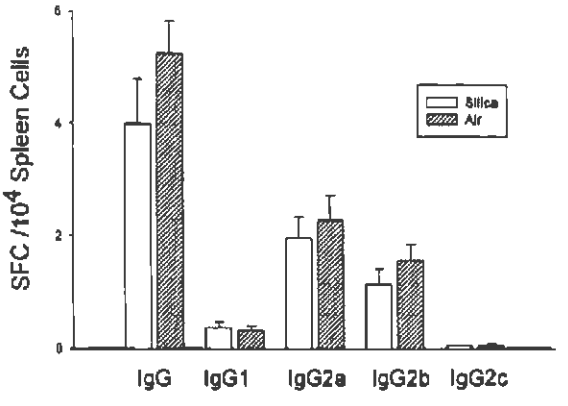

FIGURE 4. IgG and IgG subclass spot-forming cells (SFC) in spleen cell populations of silica- and air-exposed rats sacrificed 3–4 months after exposure. Each bar represents mean ± SEM of fiveexperiments. *Silica and air groups different ($p < 0.05$).

Discussion

In order to examine the relationships between experimental silicosis and dysregulated immunoglobulin production, we used a rat model that has been documented to be a good approximation of human silicosis.[22,22] In this model, rats develop silicotic changes in lung and LALN over a period of months after either quartz or cristobalite aerosol inhalation. We have previously reported that the model is also associated with elevations in serum IgG, which is a prominent feature of immune dysregulation occurring in humans exposed to silica.[13] The current study confirms these findings, as silica-exposed rats exhibited significant increases in both serum IgG and IgG-SFC per 10^4 LALN and lung cells. The increase in total IgG-SFCs per LALN was especially impressive, as there was a 24-fold increase per 10^4 LALN cells and a 32-fold increase in total LALN cells, suggesting a 768-fold increase in IgG-SFC per LALN.

In humans, mice, and rats, total IgG can be divided into 4 subclasses. Nomenclature used to describe these subclasses can be misleading, because names used to describe the subclasses do not imply any sort of homology in structure or function with other species. The pattern of IgG subclass production in each of these species is influenced by T cells and their cytokines. Based on differing patterns of cytokine secretion, two types of T_{Helper} cell subsets have been identified: T_H1 and T_H2.[23] T_H1—but not T_H2—cells produce IL-2, IFN-γ, and lymphotoxin (TNF-β). T_H2—but not T_H1—cells produce IL-4, IL-5, IL-6, and IL-10. In humans, IL-4 supports production of IgE and IgG4; IL-10 may act as a switch factor for IgG1 and IgG3; and IFN-γ supports IgG2 production.[14,15,24] In mice, IL-4 supports production of IgG1 and IgE, while IFN-γ supports production of IgG2a and IgG3.[15]

The effects of T_H1 and T_H2 responses on B-cell class switching and production of the various IgG subclasses in rats is less well characterized than in humans or mice.[16,17] As already noted, the names of the four rat IgG subclasses (IgG1, IgG2a, IgG2b, and IgG2c) do not imply any sort of homology with the four IgG subclasses of mice (IgG1, IgG2a, IgG2b, IgG3). On the basis of patterns of antigen responsiveness, it has been proposed that mouse IgG1 correlates with rat IgG2a, mouse IgG2(a+b) correlates with rat IgG2b, and mouse IgG3 correlates with rat IgG2c.[25]

Rat IgG1 does not have a pattern of antigen responsiveness correlating with any of the murine IgG subclasses.[25] However, published data strongly suggest that production of rat IgG1 is supported by T_H2 responses and suppressed by T_H1 responses. In one report, IL-12 treatment in vivo, which promotes T_H1 responses and suppresses T_H2 responses, suppressed IgG1 alloantibody responses to blood transfusion. Furthermore, treatment of recipient rats with neutralizing anti-IFN-γ antibody abrogated suppression of IgG1 responses.[17] In another report, treatment of rats with IL-10 in vivo, which promotes T_H2 responses and suppresses T_H1 responses, upregulated IgG1 antibody responses to bovine peripheral nerve myelin in a model of experimental autoimmune neuritis (EAN).[16] Thus, current evidence strongly suggests that production of IgG1 in the rat depends upon T_H2 activation. We found an 18-fold increase in IgG1-SFC per 10^4 LALN cells in silica-exposed rats, suggesting increased T_H2 effect in vivo.

As already noted, rat IgG2a has been proposed to correlate with mouse IgG1.[25] Because mouse IgG1 production is supported by T_H2 cells and cytokines, by analogy one might expect rat IgG2a to be similarly regulated. However, current evidence suggests that regulation of rat IgG2a production is more complicated, requiring both IL-4 and IFN-γ for optimal production of IgG2a to occur. Requirement for IL-4 is suggested by in vitro studies where LPS plus IL-4 was able to reconstitute IgG2a production by B cells derived from T cell-immunodeficient rats.[26] Requirement for IFN-γ is suggested by experiments showing that in vivo treatment with neutralizing anti-IFN-γ antibody decreases IgG2a alloantibody responses to blood transfusion.[17] Furthermore, in a model of EAN, treatment with IL-10 decreases IgG2a responses to bovine peripheral nerve myelin.[16] We found that IgG2a-SFC from the LALN of silica-exposed rats were increased 10-fold, a situation compatible with the presence of both IL-4 and IFN-γ sufficient for increased production of this IgG subclass.

Rat IgG2b and IgG2c production appear to be preferentially supported by T_H1 cells and IFN-γ. Treatment with IL-12 has been found to markedly increase IgG2b and IgG2c alloantibody responses to blood transfusion.[17] In the case of IgG2b, treatment with neutralizing anti-IFN-γ antibody partially blocked the IL-12 effect. In the case of IgG2c, treatment with neutralizing anti-IFN-γ antibody completely blocked the IL-12 effect. In the current study, we found a 28-fold increase in IgG2b-SFC and an 8-fold increase in IgG2c-SFC per 10^4 LALN cells, suggesting induction of a T_H1 effect in vivo.

Conclusions

In summary, the current study confirms the presence of increased serum IgG in experimental silicosis and is consistent with LALN and lung as sites for increased IgG production. Furthermore, the pattern of IgG subclass production occurring in LALN of silica-exposed animals does not suggest that increased IgG production is the result of only T_H1 or T_H2 lymphocyte activation. Instead, the pattern of IgG subclass production is consistent either with activation of both T_H1 and T_H2 responses; or induction of responses such as cytokine networking that augment production of both T_H1- and T_H2-dependent IgG subclasses by B cells; or both. In this regard, a number of cytokines that cannot be categorized by the T_H1 or T_H2 scheme but can markedly affect immunoglobulin production by B cells (such as IL-1β, TNF-α, IL-6, and TGF-β) are important participants in the cytokine networking induced by silicosis.[5,8,27-30]

References

1. Anonymous. Silicosis and silicate disease committee. Diseases associated with exposure to silica and nonfibrous silicate minerals. Arch Pathol Lab Med 1988; 112:673–720.
2. Adamson IYR. Radiation enhances silica translocation to the pulmonary interstitium and increases fibrosis in mice. Environ Health Perspect 1992;97: 233–238.
3. Velan GM, Kumar RK, Cohen DD. Pulmonary inflammation and fibrosis following subacute inhalational exposure to silica: determinants of progression. Pathology 1993;25:282–290.
4. Weissman DN, Banks DE. Silicosis and coal workers' pneumoconiosis. In: Schwarz MI, King TE, editors. Interstitial lung disease. Malden MA: B.C. Decker; 1998: 325–350.
5. Davis GS. Pathogenesis of silicosis: current concepts and hypotheses. Lung 1986;164.

6. Li W, Kumar RK, O'Grady R, Velan GM. Role of lymphocytes in silicosis: regulation of secretion of macrophage-derived mitogenic activity for fibroblasts. Int J Exp Pathol 1992;73:793–800.
7. Sjostrand M, Absher PM, Hemenway DR, Trombley L, Baldor LC. Comparison of lung alveolar and tissue cells in silica-induced inflammation. Am Rev Respir Dis 1991;143:47–52.
8. Vanhee D, Gosset P, Boitelle A, Wallaert B, Tonnel A. Cytokines and cytokine network in silicosis and coal workers' pneumoconiosis. Eur Respir J 1995;8: 834–842.
9. Anonymous. American Thoracic Society. Adverse effects of crystalline silica exposure. Am J Respir Crit Care Med 1997;155:761–765.
10. Davis GS, Pfeiffer L, Hemenway DR. Expansion of interferon-gamma-producing lung lymphocytes in mouse silicosis. Am J Respir Cell Mol Biol 1999;20: 813–824.
11. Davis GS, Pfeiffer L, Hemenway DR. Interferon-gamma production by specific lung lymphocyte phenotypes in silicosis in mice. Am J Respir Cell Mol Biol 2000;22:491–501.
12. Garn H, Friedetzky A, Kirchner A, Jager R, Gemsa D. Experimental silicosis: a shift to a preferential IFN-γ-based Th1 response in thoracic lymph nodes. Am J Physiol Lung Cell Mol Physiol 2000;278:L1221–L1230.
13. Huang SH, Hubbs AF, Stanley CF, Valliathan V, Schnabel PC, Rojanasakul Y, Ma JK, Banks DE, Weissman DN. Immunoglobulin responses to experimental silicosis. Toxicol Sci 2001;59:108–117.
14. Banchereau J, Bazan F, Blanchard D, Briere F, Galiza JP, Van Kooten C, Liu YJ, Rousset F, Saeland S. The CD40 antigen and its ligand. Annu Rev Immunol 1994; 12:881–922.
15. Snapper CM, Mond JJ. Towards a comprehensive view of immunoglobulin class switching. Immunol Today 1993;14:15–17.
16. Bai XF, Zhu J, Zhang GX, Kaponides G, Hojeberg B, van der Meide PH, Link H. IL-10 suppresses experimental autoimmune neuritis and down-regulates T_H1-type immune responses. Clin Immunol Immunopathol 2001;83:117–126.
17. Gracie JA, Bradley JA. Interleukin-12 induces interferon-gamma dependent switching of IgG alloantibody subclass. Eur J Immunol 1996;26:1217–1221.
18. Lantz RC, Stanley C, Hinton DE. Development of alteration in the lung induced by inhaled silica: a morphometric study. Publication 1986. Washington DC: Generic Mineral Technology Center for Respirable Dust, Office of Mineral Institutes, US Bureau of Mines; 1989, 289–292.
19. Lycke NY, Coico R. Measurement of immunoglobulin synthesis using the ELISPOT assay. In: Coligan JE, Kruisbeek AM, Margulies DH, Shevach EM, Strober W, editors. Current protocols in immunology. New York: Wiley, 1996:7.14.1–7.14.9.
20. Bice DE, Harris HL, Schnizlein CT, Mauderly JL. Methods to evaluate the effects of toxic materials deposited in the lung on immunity in lung-associated lymph nodes. Drug Chem Toxicol 1979;2:35–47.
21. Absher MP, Trombley L, Hemenway DR, Mickey RM, Leslie KO. Biphasic cellular and tissue response of rat lungs after eight-day aerosol exposure to the silicon dioxide cristobalite. Am J Pathol 1989;134: 1243–1251.
22. Mohr C, Davis GS, Graebner C, Hemenway DR, Gemsa D. Enhanced release of prostaglandin E2 from macrophages of rats with silicosis. Am J Respir Cell Mol Biol 1992;6:390–396.
23. Romagnani S. T-cell subsets (Th-1 versus Th-2). Ann Allergy Asthma Immunol 2000;85:9–21.
24. Wilkes DS, Heidler KM, Niemeier M, Schwenk GR, Mathur PN, Breite WM, Cummings DW, Weissler JC. Increased bronchoalveolar IgG2/IgG1 ratio is a marker for human lung allograft rejection. J Invest Med 1994; 42:652–659.
25. Der Balian GP, Slack J, Clevinger BL, Bazin H, Davie JM. Subclass restriction of murine antibodies III. Antigens that stimulate IgG3 in mice stimulate IgG2c in rats. J Exp Med 1980;152:209–218.
26. Sakai T, Agui T, Muramatsu Y, Nagasawa H, Himeno K, Matsumoto K. Low level of immunoglobulin G2a subclass correlates with a deficiency in T helper cell function in LEC mutant rats. J Vet Med Sci 1995;57: 527–529.
27. Garn H, Friedetzky A, Davis GS, Hemenway DR, Gemsa D. T-lymphocyte activation in the enlarged thoracic lymph nodes of rats with silicosis. Am J Respir Cell Mol Biol 1997;16:309–316.
28. Huaux F, Louahed J, Hudspith B, Meredith C, Delos M, Renauld JC, Lison D. Role of interleukin-10 in the lung response to silica in mice. Am J Respir Cell Mol Biol 1998;18:51–59.
29. Jagirdar J, Begin R, Dufresne A, Goswami S, Lee T, Rom W. Transforming growth factor-fl in silicosis. Am J Respir Crit Care Med 1996;154:1076–1081.
30. Piquet P, MACollart, Grau J, Sappino A, Vassalli P. Requirement of tumour necrosis factor for development of silica-induced pulmonary fibrosis. Nature 1990;344:245–247.